

Understanding shallow landslides in Campos do Jordão Municipality – Brazil: disentangle the anthropic effects from natural causes in the disaster of 2000

Rodolfo M. Mendes¹, Márcio Roberto M. de Andrade¹, Javier Tomasella¹, Márcio Augusto E. de Moraes¹, Graziela B. Scofield¹

¹National Center for Monitoring and Early Warning of Natural Disasters, Parque Tecnológico/São José dos Campos, Estrada Doutor Altino Bondesan 500,12247-016, São Paulo, Brazil

Correspondence to: Rodolfo M. Mendes (rodolfo.mendes@cemaden.gov.br)

Abstract. Located in a mountain area of Southeast Brazil, the municipality of Campos do Jordão has been hit by several landslides in recent history. Among those events, the landslides of early 2000 were significant for the number of deaths (10), the population affected and the destruction of infrastructure that caused. The purpose of this study is to assess the relative contribution of natural and human factors in triggering the landslides of the 2000 event. To achieve this goal, a detailed geotechnical survey was conducted in three representative slopes of the area to obtain geotechnical parameters needed for slope stability analysis. Then, a set of numerical experiment with Geo-Slope software was designed including natural and anthropic factors separately. Results showed that natural factors, thus is, high intensity rainfall and geotechnical conditions, were not severe enough to trigger landslides in the study area and that human disturbance were entirely responsible for the landslides events of 2000. Since the anthropic effects used in the simulations are typical of Brazilian hazardous urban areas, we concluded that the implementation of public policies that constrain the occupation of landslide susceptible areas are urgently needed.

1 Introduction

Due to the combination of frequent heavy rain of high intensities on landscapes dominated by narrow valley and steep slopes, large areas of the southeast and south of Brazil are naturally susceptible to landslides. In addition, population growth, increased urbanization, recent estimations (CEPED 2012) indicates that more than 160 million inhabitants live in urban areas (about 90% of Brazilian population), and expansion of urban construction into hazardous areas have led to an escalating impact of this natural disaster. Consequently, landslides are directly associated with loss of lives, property and infrastructure damage, and environmental destruction. During 2011, for instance, mountainous regions of Rio de Janeiro State suffered several landslides that caused more than 1,500 deaths and severe damage to the urban and rural infrastructures (Coelho Netto et al., 2013).

29 In spite of floods (generally gradual flooding) being the most disrupted natural disasters in terms of economic damages and
30 population affected, landslides have been considered the most severe in terms of dead toll (Londe et al., 2014). Although
31 landslide and flashfloods usually affect heavily urbanized downtown areas, it is also recognize that poor population living in
32 the outskirts are more vulnerable to these types of disaster. Increased landslide hazard, for instance, has been related to the
33 improper cut-and-fill construction of self-built housing on steep slopes, after the removal of vegetation. In addition, because
34 of the lack of collection systems, sewage is disposed into the hillslope soils further increasing the risks of triggering
35 landslides, not to mention the health risks associated with the lack of sanitation.

36 Among those areas affected by landslides in SE Brazil, the municipality of Campos do Jordão has been hit by several events
37 since the seventies. The most recently severe landslides occurred in the early days of 2000, leaving 103 people injured, 10
38 fatalities, and more than 423 houses at risk of collapse (Londe et al., 2014).

39 Early warning system used by the civil defense in Campos do Jordão and by CEMADEN (National Center for Monitoring
40 and Early Warning of Natural Disasters) are based on threshold values of 72 h accumulated rainfall, derived from empirical
41 studies (Tatizana et al., 1987; Santoro et al., 2010). In 2000, rainfall was monitored every 24 h at 7:00 am using manual rain-
42 gauges, and the threshold value for triggering landslides were based on previous studies in other areas of Brazil. Since the
43 accumulated rainfall values responsible for the occurrence of the landslides of 2000 were well below the critical line
44 proposed in previous studies (Tatizana et al., 1987), it was not possible to conduct the pre-emptive evacuation of many
45 hazardous areas.

46 Although empirical rainfall thresholds are successfully used in operational warning systems to predict shallow landslides
47 (Lagomarsino et al., 2013), critical rainfall thresholds for triggering landslides vary due to regional and local precipitation
48 distribution, slope morphometry, soil characteristics, lithology, microclimate and geological history (Crosta, 1998; Van Asch
49 et al., 1999). Therefore, the reliability of empirically derived critical rainfall threshold depends entirely on the availability of
50 a significant number of cases relating the occurrence of landslides and rainfall conditions. In this sense, Guzzetti et al. (2007)
51 lists as regional thresholds those covering regions with a few to many thousands square kilometers and having similar
52 meteorological, climatic and physiographic characteristics, whereas for local conditions the geomorphology and climate
53 regime are considered to be applicable to areas that range in the order of hundreds of square kilometers.

54 After the event of 2000, new critical 72 h rainfall thresholds values for landslides were proposed for the area. In addition, the
55 Civil Defense of the State of São Paulo established new critical rainfall amounts for visually monitoring critical areas in
56 order to detect early signals that may indicate the imminence of a landslide. However, the peak rainfall intensities recorded
57 in the event of 2000 did not repeat even since, while irregular occupations continued in many landslide prone areas.
58 Therefore, a detailed study of the event of 2000 is relevant not only because it's extreme characteristics, but also with the
59 perspective that memory of the 2000 event is dim and its impacts is largely underestimated among many local residents.

60 In this context, for a limited number of data hydrologic models are relevant for investigating precipitation induced shallow
61 planar landslides (Terlien, 1998).

62 Given the lack of detailed data from historical landslides events in the municipality of Campos do Jordão, the aim of this
63 study was to understand the factors responsible for triggering the landslides of early 2000 in the area using a numerical
64 model that fully couple slope stability analysis with saturated/unsaturated transient pore-water pressure simulations.
65 Physical-based hydrological models have been widely applied to predict pore-pressure build-up due to the infiltration in
66 shallow landslides (Fratini et al., 2009; Iverson, 2000). Several models, based on the infinite slope concepts, that integrates
67 hillslope hydrology with slope stability, are reported in literature: for instance SINMAP (Pack et al, 1998), SHALSTAB
68 (Dietrich et al., 1998), TRIGRS (Baum et al., 2002) and GEOtop-FS (Rigon et al., 2006).
69 During the last decade, physically based landslide prediction models have also been successfully used in early warning
70 systems. Models used in such applications include, among others, the Combined Hydrology and Stability Model-CHASM
71 (Thiebes et al, 2014), the High Resolution Slope Stability Simulator -HIRELESS (Rossi et al, 2013); the SLOPE-Infiltration
72 Distributed Equilibrium-SLIDE (Liao et al, 2010; Montrasio and Valentino, 2008), the Shallow Landslides Instability
73 Prediction-SLIP (Montrasio 2000; Montrasio et al, 2011). Another slope stability model is the modular software package
74 GeoStudio (2012), in which SEEP/W and SLOPE/W plugins are used to simulate the instability of slopes during extreme
75 rainfalls. Although GeoSlope is a simplified "single slope" model, it has been used in several previous studies to understand
76 the effect of infiltration on rainfall-induced landslides (for instance Ng and Shi, 1998; Gasmo et al., 2000; Kim et al., 2004;
77 Huat et al., 2006; Oh and Vanapalli, 2010; Acharya et al., 2016), producing very good results (Tofani et al., 2006).
78 In this study, we analyzed several scenarios that included the relative influence of natural and anthropic factors that prevails
79 in the area, and identified the most critical factors responsible for the severe landslides of 2000 using the GeoStudio (2012)
80 software due to its versatility of for handling natural and anthropic boundary conditions separately.
81 In addition, we analyzed if the threshold rainfall values establish by the Civil Defense are adequate for early warning of
82 landslides occurrence taking into account the today's occupation patterns of landslide prone areas.
83

84 **2 Material and Methods**

85 **2.1 Study site**

86 The study site is the municipality of Campos do Jordão, of the State of São Paulo, located in a mountainous region along the
87 Mantiqueira Hills (Figure 1). In geological and geomorphological terms, the Campos do Jordão plateau is a crystalline
88 plateau block with elevations of more than 2,000 m above sea level and bordered by steep cliffs that rise approximately
89 1,500 m over the adjacent Paraíba valley (Almeida, 1976). The relief, strongly conditioned by the structures and lithologies
90 of the area, is characterized by the presence of high hills and erosion of grandstands. On the basis of these amphitheaters
91 occur peat depressions (Modenesi-Gauttieri and Hiruma, 2004), where deposits of organic clay of varying thickness are
92 found. The geological and geotechnical characteristics of the deposits of organic clay and its quite sensitive behavior to

93 sudden human interventions that alter their original equilibrium conditions have conditioned the slopes stability in the urban
94 area of the municipality of Campos do Jordão (Ogura et al., 2004).

95 The area where Campos do Jordão is located was occupied by Portuguese settlers during the XVIII century. During the
96 hygienist movement (late XIX and early XX centuries), various health facilities were established in the town, mainly for
97 tuberculosis treatment. Since 1940, the town experienced a large population growth and urban expansion due to the
98 development of tourism: the number of inhabitants increased from 13 thousand in 1950 to more than 50 thousand according
99 to the estimates, with density of 164.76 pop/Km², 99.3% of which live in the urban area (IBGE, 2016).

100 The process of accelerated urbanization, specially from the 70s, of areas with unfavorable geotechnical characteristics, has
101 been pointed out as responsible for most of the natural disasters in Campos do Jordão (Ridente et al., 2002). Table 1 shows
102 the most important events in terms of dead toll and damages recorded in the area.

103 Landslides in the study area are classified as shallow, translational type, with depths of the rupture surfaces less than 2 m.
104 Depending on the position of the rupture, three different processes are observed: the rupture surface occurs in the residual
105 soil of undisturbed ground; the rupture surface occurs in the residual soil of a slope cut; and the rupture surface occurs in the
106 base of the landfill deposit, or in the slope residual soil with mobilization of the overlying landfill. The last landslide types
107 are more harmful since they mobilized larger amounts of material. In the case of the event of 2000 (Figure 2), which is the
108 focus of this study, rainfall began on 31/12/1999, and continued almost uninterrupted for 4 days with high intensity rainfall
109 bursts. According to the Brazilian Center for Weather forecasting and Climate Study – CPTEC, daily rainfall from
110 31/12/1999 through 05/01/2000 was, respectively, 78.5, 101, 120, 60, 144.5 and 10.5 mm (Ridente et al., 2002). Landslides
111 associated with this event, were considered to be one of the most severe in urban areas in Brazil, since hundred of landslides
112 occurred, mostly in slopes in poor neighborhoods where houses are constructed over cut-and-fill areas.

113 Based on the landslides events of 1972, 1991 and 2000, Ridente et al. (2002) proposed an approximation of the critical
114 rainfall necessary for the deflagration of landslides in Campos do Jordão, revealing that, in most cases, landslides are due to
115 occur after three-day rainfalls of about 200 mm, with a daily rainfall of at least 70 mm during the last day analysed. The
116 Civil Defense Preventive Plan of the State of São Paulo uses three indexes of precipitation accumulated in three days (60, 80
117 and 100 mm) as critical thresholds to enter into warning level (Santoro et al., 2010). These thresholds were based on the
118 studies carried out by Tatizana et al. (1987) and has been considered a critical value for issuing early warnings based on
119 rainfall observation and forecasting.

120 Aiming to develop relationships for the prediction of mass movements in the area, Ahrendt (2005) attempted to correlate
121 precipitation with the occurrence of landslides based on the critical intensity curves obtained by Tatizana et al. (1987) for
122 Serra do Mar in the municipality of Cubatão, and by D'Orsi (1997) for Serra da Mantiqueira in the Municipality of Rio de
123 Janeiro. Results showed that the occurrences of Campos do Jordão were below the critical lines of those areas, indicating
124 that the rainfall intensities required for triggering landslides in Campos do Jordão are much lower if compared to the other
125 sites. Therefore, the study of Ahrendt (2005) concluded that rainfall characteristics that triggers landslides in Campos do
126 Jordão are very unique and a different and more detailed approach was needed.

127 Considering the limited historical data of landslide occurrences and the few previous studies in the area that makes extremely
128 difficult to define accurate critical threshold rainfall values that triggers landslides, in particularly, the effects the
129 accumulated rainfall on the water movement and its relationship to rapid mass movements.
130 The Brazilian National Centre for Monitoring and Early Warnings of Natural Disasters – CEMADEN began to monitor
131 Campos do Jordão by the summer of 2012. Most of the occurrences were observed in cut-and-fill slopes, with evident
132 contribution of wastewater and micro drainage deficiency. Recent history did not recorded occurrences of great magnitude;
133 however, the destruction, or even the prohibition of occupying damaged houses, is a recurrent problem.

134

135 **2.2 Soil moisture monitoring**

136 Soil moisture was monitored in every hourly interval to a depth 3.0 meters along the 12 months (01/01/2016 to 12/31/2016),
137 using two EnviroScan™ probes installed next of the borehole SD-03 (Figure 3). EnviroScan™ probes are installed into
138 customized access tubes manufactured by Sentek Pty. Ltd. Inside of the EnviroScan™ probe were distributed six Sentek
139 capacitance sensor. The capacitance sensor gives an output in volumetric water content (mm of water per 100 mm of soil
140 measured). This is converted from a scaled frequency reading using a default calibration equation, which is based on data
141 obtained from numerous scientific studies in a range of soil textures.

142 Before a Sentek capacitance sensor can be installed in the soil, it must have minimum and maximum values set. This is done
143 using air and water around each sensor (lecture limits of the volumetric water content – dry and saturated, respectively).

144 Soil moisture was monitored during 2016 at hourly intervals and to a depth of 3.0 m using two EnviroScan™ (Campbell
145 Scientific, 2016) probes installed next of the borehole SD-03 (Figure 2). Each probe included six capacitance sensors that
146 measured soil moisture every 0.5 m, thus is, at the depths of 0.5, 1.0, until 3.0 m deep, which allowed to monitor moisture
147 variations of the landfill, residual and saprolite layers. Before the EnviroScan™ capacitance probes were installed in the
148 soil, maximum and minimum values were normalized by matching the raw readings from each sensor at both 0% (held in
149 air) and 100% water levels (submerged in water).

150 2.3 Geotechnical survey

151 SPT (Standard Penetration Test) boreholes were drilled along three profiles of the study site (A-A'; B-B'; C-C' in Figure 3) at
152 six different positions along the slopes (SD-01 to SD-6, Figure 4). Disturbed and undisturbed samples were taken from the
153 boreholes for the determination of the parameters used for stability analysis.

154 Three (03) undisturbed samples were collected in migmatitic saprolite block close to the SD-04 borehole. This material
155 occurs anisotropically and discontinuously, because it presents significant textural variation resulting from the heterogeneity
156 of the parental rock, being predominantly formed by silt and fine sand, with variable occurrence of clay. From the 6
157 boreholes (SD-1 to SD-6) and the 3 undisturbed blocks it was possible to obtain a total of 12 soil samples to perform
158 geotechnical characterization tests of the study area following Brazilian standard procedure.

159 Disturbed and undisturbed samples collected were used to perform grain size analysis test (ABNT, 1984b and 1995), soil
160 particle density (ABNT, 1984a), bulk density, specific dry mass and Atterberg limits (ABNT, 1984c and 1984d). Parameters
161 of effective cohesion (c') and effective friction angle (ϕ') were obtained from saturated direct shear tests, using square
162 shaped undisturbed samples with 60 mm of side and height of 25 mm. The soil samples were in their natural state, being
163 representative of the "Residual" and "Saprolite" soil layers. During the consolidation step, all specimens were saturated for
164 24h and subjected to net normal stresses of 25, 50 and 100 kPa. Then, in the shearing phase, a constant velocity of 0.033 mm
165 min^{-1} was applied. Vertical and horizontal displacements were recorded during the consolidation and shearing phases.

166 After saturation soil samples for 12 hours, Water Retention Curves - WRC of the residual soils layers were obtained using
167 pressure plate for suctions <100 kPa and filter paper for suctions ≥ 100 kPa for the drying path of the samples following the
168 recommendation of Marinho and Oliveira (2006). Results showed that the differences of water retention values at the
169 transition among both method were not significant, making unnecessary further adjustments (Figure 8). The saturated
170 hydraulic conductivity - K_{sat} was obtained in laboratory using a constant head permeameter. Hydraulic conductivity
171 functions were estimated from the WRC, K_{sat} using the Van Genuchten (1980) model. In the case of landfill deposits, the
172 values of K_{sat} for different soil texture were those obtained Ahrendt (2005) from core measurements.

173

174 2.4 Modelling experiments

175 The modelling of the stability and seepage analysis was divided in two parts: (1) transient unsaturated seepage analysis; (2)
176 stability analyses coupled with the results from the previous step.

177 For the seepage analysis, 35-days accumulated rainfall of the period 01/12/1999 through 04/01/2000 was considered, since
178 that event triggered several landslides in the study area (Ahrendt and Zuquette, 2003). In addition to the geotechnical
179 parameters, anthropic factors that induce landslides typical of Brazilian urban slopes, specifically housing load, man-made
180 cuts and leakage from pipes, were included in the modelling experiment with the aim of analysing the degree of influence of
181 these factors on the trigger of landslides in the study area during 2000 (Figures 4, 5 and 6).

182 The boundary conditions were set according to field observations on the landslide area and boundary conditions used by
183 Rahardjo et al. (2007). The non-saturated transient flux results were obtained for two cases: considering only the
184 accumulated rainfall and rainfall including linear leakage along the cut slope (Figure 5). The initial pore-pressure values used
185 in the transient flow analysis were obtained indirectly from the WRC and the data of the soil moisture sensors installed in the
186 study area (Figures 8 and 7). Next, the factor of safety (FS) for the slope was estimated from the transient seepage modelling
187 coupled with the stability analysis tool (Geo-Slope, 2012a). All the stability analyses were conducted considering the theory
188 of static equilibrium of forces and momentum. The FS were calculated using the geotechnical and anthropic parameters,
189 obtained from the method of Morgenstern-Price, which considers circular and non-circular rupture surfaces. All the
190 simulations allowed the slope stability module SLOPE/W to identify the most critical rupture surface (Figure 6). Therefore,
191 the values of the Slope Safety Factor – FS, were the lowest of all conditions analysed.
192

193 3 Results

194 3.1 Geotechnical survey

195 The result of the granulometric analyses of the residual and saprolite layers of the three profiles studied are presented in
196 Figure 7. Residual layer (sample SD-01/2.0 m) can be classified as clayey sand, with percentage of sand and silt of 53 % and
197 25 %, respectively. The soil samples representative of the saprolite layer showed a significant variation of the percentage of
198 the clay fraction (3 to 24%), silt (14 to 42%) and sand (53 to 73%), indicating that soil profiles are heterogeneous, which in
199 agreement with the textural characteristics of its parent material (migmatitic gneiss). Therefore, it is expected that the
200 mechanical and hydraulic properties of this soil layer present high variability. The general results of the geotechnical tests
201 (general characteristics, shear strength and saturated hydraulic conductivity) of the samples of the representative soils of the
202 studied area are presented in Table 2.

203 Analysing the values of the effective strength parameters (c' and ϕ') and saturated hydraulic conductivity (Table 2), the
204 values representative of the 'Saprolite' layer showed significant variability: the coefficient of variation was 85% for the
205 effective cohesion; 20% for the effective friction angle, and 89% for the saturated hydraulic conductivity, reflecting the
206 heterogeneity character of the parent material. The high values of the resistance parameters shown in Table 2 are associated
207 with the high heterogeneity of the residual gneiss soil, such as the presence quartz particles and other minerals of
208 considerable size in the specimens tested, which confer them high resistance. In addition, the values of the resistance and
209 K_{sat} parameters obtained in this study are close to mean reference values of residual gneiss soils representative of other
210 Brazilian sites (Costa Filho and Campos, 1991; Ahrendt, 2005; Reis et al., 2011).

211 Figure 8 shows the water retention curves of the soil layers representative of the profiles. In general, the residual and
212 saprolite layers are able to hold more water compared to the landfill deposit. For example, for a field matrix suction level of

213 100 kPa, the volumetric moisture values of the Landfill Deposit, Residual Soil and Saprolite layers are, respectively, 0,06
214 m^3/m^3 ; 0,24 m^3/m^3 ; 0,26 m^3/m^3 .

215

216 **3.2 Soil moisture data**

217 Soil moisture data from 2016 from the EnviroScanTM probes (3G1 and 3G2) are presented in **Figure 9**. The data from 3G1
218 (upper graph of **Figure 9**) showed that the sensor installed at a lower depth (0.5 to 1.0 meter), representative of the landfill
219 deposit (green curve) layer, have variations larger soil moisture variations ($\Delta\theta = 32\%$), with maximum and minimum water
220 content values recorded in March (46%) and April (14%), respectively. At deeper layers (1-3 meters deep), representative of
221 the "Residual" and "Saprolite" layers (black and red curves), time variation of soil moisture is much lower ($\Delta\theta = 10\%$, on
222 average). In the Residual layer (black curve), maximum and minimum values of soil moisture were verified in January
223 (38%) and May (27%), respectively. In the case of the saprolite layer (red curve) maximum and minimum humidity values in
224 the months of June (40%) and May (32%). The different dynamics among the three soil layers are reflecting not only
225 differences in the retention properties of each layer considered but also the deep soil water dynamics down the soil profiles.
226 This explains why the upper layer (landfill deposit) shows a more spiky behaviour in response the rainfall; while the other
227 two layers exhibit gradual and delayed variations related to deep water percolation.

228 Analysing the data of the probe 3G2 (lower graph of Figure 9), it is clear that the soil moisture variation of the sensor of the
229 surface layer, representative of the Landfill Deposit layer (green curve), was significantly lower ($\Delta\theta = 15\%$) compared to the
230 same layer of probe 3G1. Maximum and minimum soil moisture values were recorded in September (43%) and August
231 (28%), respectively. At deeper depth, within the residual and saprolite layers (black and red curves), time variation of soil
232 moisture variation is similar than the measurements of probe 3G1 ($\Delta\theta = 9\%$, on average). For the "Residual" layer (black
233 curve) maximum and minimum soil moisture values were observed in January (31%) and May (21 %), respectively; while in
234 the "Saprolite" layer (red curve) maximum and minimum soil moisture values in the months of January (37%) and August
235 (30%).

236 **Contrasting differences in the soil moisture behaviour of the landfill deposit from the probes 3G1 and 3G2 suggest that the**
237 **variability of soil parameters is higher in the top layer. This was expected considering that this layer is the result of the cut-**
238 **and-fill processes mixed with construction wastes of several types.**

239 **3.3 GeoSlope simulations input data**

240 Table 3 summarizes the parameters used in the numerical simulation with GeoSlope software, based on the geotechnical
241 survey and information extracted from different sources.

242 Regarding the geotechnical properties, in order to reduce the uncertainties due to the heterogeneity of the parent material, the
243 mean values of the resistance (c' and ϕ'), bulk density and saturated hydraulic conductivity parameters for saprolite and
244 residual (Table 2) were used in the flow and stability modelling. As mentioned before, for the landfill deposit, the
245 geotechnical parameters were those obtained by Ahrendt (2005).

246 Based on the field information from previous studies in Brazil, the anthropic factors considered in the simulations were:
247 point leakage sources of $1.0 \text{ m}^3 \text{ day}^{-1}$ (SABESP, 1993 and 2016) for simulation that include leakage; distributed load due to
248 one floor housing of 2.0 kNm^{-2} (ABNT, 1980); height of the cutting slope (based on field data). In the case of the simulations
249 that include leakage, one point of leaking constant value of $1.0 \text{ m}^3 \text{ day}^{-1}$ was considered in the cut slope, after the 10th day of
250 the simulation until the 35st day, since numerical experiments showed that a time interval of 10 days was adequate to
251 minimize the effect of the uncertainties of initial pore-pressure conditions used in the simulations. It should be noted that this
252 strategy helped to separate the effect of leakage from other anthropic factors, without impacting the results at the end of the
253 simulation period (day 35).

254 For the transient flow analysis, the highest average moisture values of the three layers was considered (Landfill deposit -
255 $\theta_{\text{mean}} = 33\%$, Residual - $\theta_{\text{mean}} = 31\%$, Saprolite - $\theta_{\text{mean}} = 34\%$, to November 30, 2016 - light red region in Figure 9).
256 Subsequently, the mean values of humidity were used to obtain the initial values of matrix suction from the representative
257 water retention curves of each layer of the profile. The proper choice of the initial values of matrix suction is to provide the
258 numerical model with a fast and coherent convergence in the pore-pressure distribution of water in the soil layers, aiming to
259 adjust them satisfactorily to the rain data considered in the flow analysis (01 From December 1999 to January 4, 2000 - 35
260 days).

261 For the transient flow analysis, the initial conditions of the simulations were derived assuming initial soil moisture values of
262 $0.33 \text{ m}^3 \cdot \text{m}^{-3}$, $0.31 \text{ m}^3 \cdot \text{m}^{-3}$ and $0.34 \text{ m}^3 \cdot \text{m}^{-3}$, for the landfill deposit, residual and saprolite layers respectively. These values
263 correspond to average of the highest soil moisture values of the two probes during November 2016, and indicated by the
264 light-red shaded area of Figure 9.

265 Subsequently, the mean moisture values were used to obtain the initial values of matrix suction from the representative water
266 retention curves of each layer of the profile (Figure 8). This choice of the initial values of matrix suction of the numerical
267 experiments proved to be crucial to achieve a fast and coherent convergence of pore-pressure distribution of soil layers in the
268 simulations, since they are representative of the 35 days period considered in the flow analysis (From 01/12/1999 through
269 04/01/2000). Based on this approach, the values of negative pore pressure (matrix suction) were -10 kPa for landfills, -40
270 kPa for residual and -40 kPa for the saprolite.

271

272 **3.4 Slope Safety Factor Analysis**

273 Figure 10 shows the time variation of the slope safety factor (FS) during 35 days for the 2000 rainfall for the three profiles.
274 In Figure 10, two "warning zones" are considered: zone of instability $\text{FS} < 1.0$, **where ruptures should occur**; and low stability
275 stable zone, $1.0 < \text{FS} < 1.5$, which indicates a low possibility of landslide occurrence. In this warning zone the Brazilian
276 Association of Technical Standards (ABNT, 1991) established the following conditions for the safety degree of the slope:
277 High ($1.3 \leq \text{FS} < 1.5$); Mean ($1.15 \leq \text{FS} < 1.3$); Low ($1.0 \leq \text{FS} < 1.15$).

278 For all three profiles analysed, it is clear that the effect of daily rain on the decrease of the FS (green line) was practically
279 insignificant, with FS values above the 1.5 threshold (high safety degree of the slope); indicating very low likelihood of
280 landslides. In the “rainfall only” scenario, the variations in FS values are due to the geotechnical and geomorphological
281 characteristics of the analysed profiles only. For the "rainfall only" scenario, the difference between FS values in the three
282 profiles are mainly due to: the surface slope, since the profile AA' is steeper than CC' which is steeper than BB'; due to
283 differences in the thickness and location of the layers along the slope (Figure 4) and; the water table profile, related to the
284 soil layers.

285 For the second scenario considered in the analysis of the stability, which includes cut-and-fill effects besides rainfall (red
286 line in Figure 10), it was verified that the effect of terrain cuts caused minor effects in the slope safety factor. Except for the
287 case of the A-A' profile, which presents the FS condition <1.5 between 32th and 35th day after the beginning of rainfall, FS
288 values were above the 1.5 threshold. However, it is important to note that, in the case of the profile A-A', the decrease of FS
289 was more pronounced than in the other profiles analysed, directly related to the positioning of the cuts considered along the
290 slopes located based on field information. The configuration of the cuts used in this profile favour the wetting of the top soil
291 layer and, consequently affected the whole profile stability.

292 The third scenario of Figure 10 (black line), where the joint influence of two anthropic factors (cut and leakage) with the
293 rainfall of 2000 was considered, and the variations in FS values are significant. For the profile A-A', FS values remained
294 below the threshold of 1.5; while in the other two profiles FS dropped below 1.5 between the 32nd and 35th days of
295 simulations in the case of the B-B' profile, and on day 17th for the C-C' profile. It should be noted that, after the 11th after
296 the beginning of simulation, FS values become sensitive to rainfall variability.

297 In addition, it can be seen in Figure 10 that the profiles B-B' and C-C' showed greater sensitivity to leakages, mainly due to
298 the geological-geotechnical characteristics, and the location of the cuts along the slopes, that favoured the decrease of the
299 matrix suction values and, therefore, induced instability in both profiles. In addition, critical condition, $FS < 1.0$, in profiles
300 A-A' and C-C' are verified between days 32nd and 35th after the beginning of simulations, in response to the significant
301 rainfall that occurred at the period.

302 Finally, in the fourth scenario of Figure 10 (light brown line), when all the anthropic factors (cut, leakage and housing loads)
303 are considered together with the daily rainfall. For most of the time, FS values remained below the threshold of 1.5 in in the
304 A-A' and B-B' profiles, while in the case of the profile C-C' only after the day 34th of the simulation. The probability of
305 landslides increased significantly ($FS < 1.0$) in all profiles from day 32 of the simulation in response to heavy rainfall at the
306 end of the period. In the case of the profile C-C' (light brown line), the inclusion of housing loads appears to provide more
307 stability to the profile, probably related to the fact that the critical failure surface estimated by the numerical model was
308 different from that assumed in the case scenario 3 (black line).

309 Based on the assessment of the slope safety factor presented in Figure 10, it is clear that the probability of landslides
310 associated to 2000 rainfall on slopes covered with natural vegetation is very low. When considering the influence of rainfall
311 in conjunction with anthropogenic factors, there was a significant decrease in the safety factors in all the profile studied,

312 although the effect varied between slopes depending on the geological-geotechnical profile characteristics, geomorphological
313 conditions, water table position and the anthropic conditions, thus is, the positioning of cuts, leakage and housing loads along
314 the slope.

315 In general, slopes became unstable ($FS < 1.0$) between 32nd and 35th after the beginning of simulations when high daily
316 accumulated values were verified. Since most of the landslide occurred on day 32nd, it follows that the model successfully
317 predicted the time were the landslides began. However, it should be noted that previous accumulated rainfall values were
318 crucial to create favourable conditions for triggering landslides as shown by Figure 10 after the 30th day from the beginning
319 of simulation.

320 Santoro et al. (2010) recommended in-situ technical surveys of urban hazardous areas after accumulated 72-hour rainfall
321 equal to 60, 80 and 100 mm (depending on the municipality), in order to identify evidences of the imminence of landslides
322 and to enforce eventual preventive removal of population. It can be seen in Figure 10 that the 72h accumulated rainfall were
323 35 mm for the day 30 after the beginning of simulation; 35 mm for the day 31; 60 mm for the day 32; 191 mm for the day
324 33. Thus, critical rainfall thresholds (60-100 mm) were exceeded between 32nd and 33th day for the events recorded in the
325 year 2000.

326 In this period, the FS in the three analyzed profiles presented the lowest values, located exactly between the "low-medium
327 security zone" ($1.0 < FS < 1.3$) and "unstable zone" ($FS < 1.0$), which shows that the "anthropic and natural factors integrated
328 analysis method" proposed in this paper successfully predicted the beginning of landslides. Although the 72h rainfall
329 threshold value proposed by Santoro et al (2010) proved to be valid for the 2000 event, results of the simulation indicated
330 that the rainfall 30 days previous to the landslides was crucial to bring FS values closer to critical levels, indicating that
331 critical value presents limitations on slopes initially drier.

332 **4 Conclusions**

333 The Geo-slope model proved to be an efficient and useful tool to predict the landslide of Campos do Jordão municipality due
334 to the rainfall event of 2000 and allowed to disentangle the effects of cut-and-fill, construction practices and pipe leakage in
335 three representative slopes of the area. The use of numerical models that perform flow and stability analyses considering the
336 simultaneous influence of natural and anthropic variables showed to be accurate for the prediction of occurrences of
337 landslides on urban slopes.

338 Regarding the rainfall critical values use in early warning system by CEMADEN and the Civil Defense for the Campos do
339 Jordão Municipality, although adequate for the event of 2000, our study show that the previous rainfall history, in
340 combination with leakages, played a fundamental role to create favorable conditions for the occurrence of landslides. This is
341 related to the fact that leakages contribute to keep the soil profile closer to saturation at the beginning of the period of more
342 intense rainfall, and consequently the developing of positive pore-pressure conditions. In other words, the threshold currently
343 used for issue early warning would result in late alarms under initial drier soil conditions, at least in heavily disturbed
344 landscapes.

345 The results of the stability analyses confirmed the hypothesis that the occurrence of landslides in the study area cannot be
346 attributed solely and exclusively to the rainfall events of the year 2000, despite the significant accumulated values.
347 Therefore, numerical modelling results corroborated the fact that the occurrence of landslides was the combination of natural
348 and anthropic factors, with the decisive influence of the latter, thus is, due to the presence of several cuts along the slope
349 combined with load of constructions and leakage. Clearly, human interventions on natural slopes play a fundamental role in
350 triggering landslides in heavily populated steep slopes surrounding urban areas.

351 Considering that the pattern of land use and construction used in the simulations is representative of most of the
352 neighborhood of Brazilian urban areas, the methodology used in this paper needs to be repeated and verified in other areas in
353 order to establish more accurate critical threshold that trigger landslides. Moreover, since the prone to landslide areas of
354 Campos do Jordão Municipality are not the most populated of Brazil compared, for instance, to the outskirts of several
355 metropolitan areas, it becomes crucial to verify whether a mosaic of site-specific rainfall thresholds is needed in heavily
356 occupied areas, rather a single regional threshold, as suggested by Segoni et al. (2014). In this context, this study
357 demonstrated the using the slope safety factor is viable for determine more accurate rainfall threshold that trigger landslides,
358 with direct impacts on the credibility of early warning systems, which relies in minimizing false alarms or premature/late
359 warnings.

360 Although the results of this study have uncertainties mainly associated with the geotechnical parameters used in the flow
361 analysis and slope stability, it is the first comprehensive analysis of the factors responsible for triggering landslide in Brazil
362 that integrates field evidence, anthropic effects, geotechnical data and numerical simulation. **Since simulations results
363 indicated that the slope safety factor FS was sensitive to the anthropic factors, future studies should combine modelling tools
364 with probabilistic analysis to consider a wider range of geological-geotechnical and anthropic parameters values to be able to
365 reproduce more general conditions that occur in the study area.**

366 Finally, considering that this work have demonstrated that the anthropic factors are the main instability factors in urban
367 slopes, it is essential that urban managers and planners promote public policies and enforce laws that restrict the occupation
368 of landslide susceptible areas. Detailed surveys to identify prone to landslide areas are essential, since many urban areas of
369 Brazil lack zoning of hazardous areas, which is essential to implement regulations. Besides this, educational campaigns
370 regarding the adoption of better construction practices and reducing piping leakage will be helpful in already consolidated
371 occupied areas.

372 **References**

- 373 ABNT - Brazilian Association of Technical Standards: Determination of the specific mass, NBR-6508. Rio de Janeiro, 8p,
374 1984a.
- 375 ABNT - Brazilian Association of Technical Standards: Loads for the buildings structures calculation, NBR 6120. Rio de
376 Janeiro, 5p, 1980.

377 ABNT - Brazilian Association of Technical Standards: Rocks and soils – terminology, NBR-6502. Rio de Janeiro, 1995.

378 ABNT - Brazilian Association of Technical Standards: Slopes stability, NBR-11682. Rio de Janeiro, 39p, 1991.

379 ABNT - Brazilian Association of Technical Standards: Soil – determination of the liquid limit, NBR 6459. Rio de Janeiro,
380 6p, 1984c.

381 ABNT - Brazilian Association of Technical Standards: Soil – determination of the plastic limit, NBR 7180. Rio de Janeiro,
382 3p, 1984d.

383 ABNT - Brazilian Association of Technical Standards: Soil – grain size analysis test, NBR-7181. Rio de Janeiro, 13p,
384 1984b.

385 Acharya, K. P., Bhandary, N. P., Dahal, R. K., Yatabe, R.: Seepage and slope stability modelling of rainfall-induced slope
386 failures in topographic hollows, *Geomatics, Natural Hazards and Risk*, 7(2), 721-746, 2016.

387 Ahrendt, A. and Zuquette, L. V.: Triggering factors of landslides in Campos do Jordão City, Brazil, *Bulletin of Engineering
388 Geology and the Environment*, 62, 231-244, 2003.

389 Ahrendt, A.: Gravitational mass movements - proposal of a forecast system: application at the urban area of Campos do
390 Jordão City-SP, Brazil. (In Portuguese), Doctoral thesis, School of Engineering of São Carlos, São Paulo University, Brazil,
391 390 pp., 2005.

392 Almeida, F F M. 1976. The system of continental rifts bordering the Santos Basin, Brazil. In: *Anais Academia Brasileira de
393 Ciências, CONTINENTAL MARGINS OF ATLANTIC TYPE, São Paulo, 1975, 48 (Suplemento): 15-26.*

394 Andrade, E.: Risk mapping associated to landslides, flood, erosion and undercutting of riverbank in municipality of Campos
395 do Jordão, São Paulo State, Brazil (in Portuguese), IG-CEDEC Technical Report number 01/2013, 4, 2014.

396 Baum, R. L., Savage, W. Z., and Godt, J. W.: TRIGRS – a FORTRAN program for transient rainfall infiltration and grid-
397 based regional slope stability analysis, US Geological Survey Open File Report 2002-424, 38 pp, 2002.

398 Beven, K. J. and Kirkby, M. J.: A physically based variable contributing area model of basin hydrology, *Hydrological
399 Sciences Bulletin*, 24(1), 43-69, 1979.

400 Burton, A. and Bathurst, J.: Physically based modelling of shallow landslide sediment yield at a catchment scale,
401 *Environmental Geology*, 35, 89–99, 1998.

402 Campbell Scientific: EnviroSCAN™ soil water content profile probes, Instruction Manual, 48p, “available at:
403 <https://s.campbellsci.com/documents/us/manuals/envirosmart.pdf>, 2016.”

404 CEDEC – Civil Defense Coordination of the São Paulo State: databases of the summer operation emergency calls from 2000
405 through 2013 (in Portuguese), São Paulo, 2013.

406 CEPED - Centro Universitário de Estudos e Pesquisas sobre Desastres. Atlas Brasileiro de Desastres Naturais 1991 – 2010:
407 volume Brasil. Florianópolis: UFSC, 2012. 127p.

408 Cho, S. E.: Infiltration analysis to evaluate the surficial stability of two-layered slopes considering rainfall characteristics,
409 *Engineering Geology*, 105, 32-43, 2009.

410 Coelho Netto, A. L., Avelar, A. S., Vianna, L. G. G., Araújo, I. S., Ferreira, D. L. C., Lima, P. H. M., Silva, A. P. A., and
411 Silva, R. P.: The extreme landslide disaster in Brazil, *Landslide Science and Practice*, 6, 377-384, 2013.

412 Costa Filho, L. M. and Campos, T. M. P.: Anisotropy of a gneissic residual soil, in: *Proceedings of the 9th Pan-American*
413 *Conference on Soil Mechanics and Foundations Engineering*, Vina Del Mar, Chile, 51-61, 1991.

414 Crosta, G.: Regionalization of rainfall thresholds: an aid to landslide hazard evaluation, *Environ Geol.*, 35, 131-145, 1998.

415 D’Orsi, R., D’Ávila, C., Ortigão, J. A. R., Dias, A., Moraes, L., and Santos, M. D.: Rio-Watch: The Rio de Janeiro Landslide
416 Watch System, in: *Proceedings of the 2nd Pan-American Symposium on Landslides*, Rio de Janeiro, Brazil, 21-30, 1997.

417 define a mosaic of triggering thresholds for regional-scale warning systems, *Nat. Hazards Earth Syst. Sci.*, 14, 2637–2648,
418 Dietrich, W. E., Asua, R. R., Orr, J. C. B., and Trso, M.: A validation study of the shallow slope stability model,
419 SHALSTAB, in the forest lands of Northern California. *Stillwater Ecosystem, Watershed and Riverine Sciences*, Berkeley,
420 59 pp, 1998.
421 doi:10.5194/nhess-14-2637-2014, 2014.

422 Frattini, P.; Crosta, G., and Sosio, R.: Approaches for defining thresholds and return periods for rainfall-triggered shallow
423 landslides, *Hydrol Process.*, 23, 1444-1460, 2009.

424 Gasmó, J. M.; Rahardjo, H., and Leong, E. C.: Infiltration effects on stability of a residual soil slope, *Computers and*
425 *Geotechnics*, 26, 145-65, 2000.

426 Geo-Slope: Seepage modeling with SEEP/W: an engineering methodology, User manual, Geo-Slope International, 199p,
427 2012b.

428 Geo-Slope: Stability modeling with SLOPE/W: an engineering methodology, User manual, Geo-Slope International, 238p,
429 2012a.

430 GeoStudio: GeoStudio Tutorials includes student edition lessons. Calgary, Alberta, Canadian: Geo-Slope International Ltd.,
431 2012.

432 Guzzetti, F.; Peruccacci, S.; Rossi, M., and Stark, C.P.: Rainfall thresholds for the initiation of landslides in central and
433 southern Europe, *Meteorology and Atmospheric Physics*, 98, 239-267, 2007.

434 Huat, B .B. K., Ali, F. H., and Rajoo, R. S. K.: Stability analysis and stability chart for unsaturated residual soil slope,
435 *American Journal of Environmental Sciences*, 2 (4), 154-160, 2006.

436 IBGE – Brazilian Institute of Geography and Statistics, social and economic data of the Brazilian citizens (in Portuguese),
437 “available at: <http://cidades.ibge.gov.br/painel>, 2016.”

438 Iverson, R. M.: Landslide triggering by rain infiltration, *Water Resour. Res.*, 36, 1897-1910, 2000.

439 Kim, J., Jeong, S., Park, S., and Sharma, J.: Influence of rainfall-induced wetting on the stability of slopes in weathered soils,
440 *Engineering Geology* ,75, 251-262, 2004.

441 Lagomarsino, D., Segoni, S., Fanti, R., and Catani, F.: Updating and tuning a regional-scale landslide early warning system,
442 *Landslides*, 10, 91–97, 2013. DOI: 10.1007/s10346-012-0376-y

443 Liao Z, Hong Y, Wang J, Fukuoka H, Sassa K, Karnawati D, Fathani F. (2010) Prototyping an experimental early warning
444 system for rainfall-induced landslides in Indonesia using satellite remote sensing and geospatial datasets. *Landslides* 7:317–
445 324. doi:10.1007/s10346-010-0219-7.

446 Londe, L. R., Coutinho, M. P., Di Gregório, L. T., Santos, L. B. L., and Soriano, E.: Water related disasters in Brazil:
447 perspectives and recommendations (in Portuguese), *Ambiente and Sociedade*, 17(4), 133-152, 2014.

448 Marinho, F. A. M., Oliveira, O. M.: The filter paper method revisited. *Geotechnical Testing Journal, ASTM*, 29(3):250-258,
449 2006

450 Modenesi-Gauttieri, MC; Hiruma, ST. 2004. A Expansão Urbana no planalto de Campos do Jordão. Diagnóstico
451 geomorfológico para fins de planejamento. *Revista do Instituto Geológico, São Paulo*, 25(1/2), 1-28, 2004.

452 Montrasio L (2000) Stability analysis of soil slip. In: Brebbia CA (ed) *Proceedings of International Conference BRisk 2000*^.
453 Wit Press, Southampton, pp 357–366

454 Montrasio L, Valentino R (2008) A model for triggering mechanisms of shallow landslides. *Nat Hazards Earth Syst Sci*
455 8:1149–1159. doi:10.5194/nhess-8-1149-2008

456 Montrasio L, Valentino R, Losi GL (2011) Towards a real-time susceptibility assessment of rainfall-induced shallow
457 landslides on a regional scale. *Nat Hazards Earth Syst Sci* 11:1927–1947. doi:10.5194/nhess-11-1927-2011.

458 Ng, C.W.W. and Shi, Q.: Influence of rainfall intensity and duration on slope stability in unsaturated soils, *Quarterly Journal*
459 *of Engineering Geology*, 31, 105-113, 1998.

460 Ogura, AT; Silva, FC; Vieira, AJNL. Zoneamento de risco de escorregamento das encostas ocupadas por vilas
461 operárias como subsídio à elaboração do plano de gerenciamento de áreas de risco da estância climática de Campos do
462 Jordão - SP. 2004. In: *Simpósio Brasileiro de Desastres Naturais, 1º, 2004, Florianópolis. Anais... Florianópolis:*
463 *GEDN/UFSC, 2004. p. 44-58. (CD-ROM).*

464 Oh, W.T. and Vanapalli, S.K.: Influence of rain infiltration on the stability of compacted soil slopes, *Computers and*
465 *Geotechnics*, 37, 649-657, 2010.

466 Pack RT, Tarboton DG, Goodwin CN (1998) *SINMAP—a stability index approach to terrain stability hazard mapping.*
467 *User’s manual. Terratech Consulting Ltd, Salmon Arm.*

468 Pack, R. T., Tarboton, D. G., and Goodwin, C. N.: The SINMAP approach to terrain stability mapping, in: *Proceedings of*
469 *the 8th Congress of the International Association of Engineering Geology, Vancouver, Canada, 21-25, 1998.*

470 Rahardjo, H., Ong, T. H., Rezaur, R. B., and Leong, E. C.: Factors controlling instability of homogeneous soil slopes under
471 rainfall, *J. Geotech. Geoenviron. Eng.*, 133 (12), 1532-1543, 2007.

472 Reis, R.M., Azevedo, R.F., Botelho, B.S., and Vilar, O.M.: Performance of a cubical triaxial apparatus for testing saturated
473 and unsaturated soils, *Geotechnical Testing Journal*, 34 (3), 1-9, 2011.

474 Ridente, J. L., Ogura, A. T., Macedo, E. S., Diniz, N. C., Alberto, M. C., and Santos, H. P.: Accidents associated to mass
475 movements that were occurred in municipality of Campos do Jordão, SP, at January 2000: technical actions after the
476 disasters (in Portuguese), IPT publications number 2815, 14p, 2002.

477 Rigon, R., Bertoldi, G., Over, T. M.: Geotop: a distributed hydrological model with coupled water and energy budgets,
478 Journal of Hydrometeorology, 7(3), 371– 388, 2006.

479 Rossi G, Catani F, Leoni L, Segoni S, Tofani V. (2013). HIRESSES: a physically based slope stability simulator for HPC
480 applications. Nat. Hazards Earth Syst Sci 13:151–166. doi:10.5194/nhess-13-151-2013.

481 SABESP: Leak tests, <http://site.sabesp.com.br/site/interna/Default.aspx?secaoId=244>, Accessed 04 Abril 2016, 2016.

482 SABESP: Water reduction program not charged, Synthetic report, Sao Paulo: Lyonnaise des Eaux Services Associés –
483 LYSA, 1993.

484 Santoro, J., Mendes, R. M., Pressinotti, M. M. N. and Manoel, G. R.: Correlation between rainfall and landslides occurred
485 during the operation of the prevention plan of civil defense in State of São Paulo, SP (in Portuguese), in: Proceedings of the
486 7th Brazilian Symposium on Geotechnical and Geoenvironmental Cartography, Maringá, Paraná, 1-15, 2010.

487 Segoni, S., Rosi, A., Rossi, G., Catani, F., and Casagli, N.: Analysing the relationship between rainfalls and landslides to
488 Tatizana, C., Ogura, A. T., Cerri, L. E. S., and Rocha, M. C. M.: Numerical modeling of the analysis of correlation between
489 rainfall and landslides applied to the slopes of the Serra do Mar in municipality of Cubatão (in Portuguese), in: Proceedings
490 of the 2nd Brazilian Congress of Engineering Geology, 237-248, 1987.

491 Terlien, M. T.: The determination of statistical and deterministic hydrological landslide triggering thresholds, Environ Geol.,
492 35, 124-130, 1998.

493 Thiebes B, Bell R, Glade T, Jäger S, Mayer J, Anderson M, Holcombe L.(2014). Integration of a limit-equilibrium model
494 into a landslide early warning system. Landslides 11:859–875. doi:10.1007/s10346-013-0416-2.

495 Tofani, V., Dapporto, S., Vannocci, P., and Casagli, N. (2006). Infiltration, seepage and slope instability mechanisms during
496 the 20–21 November 2000 rainstorm in Tuscany, central Italy, Nat. Hazards Earth Syst. Sci., 6, 1025–1033,
497 doi:10.5194/nhess-6-1025-2006.

498 Van Asch, T. W. J., Buma, J., and Van Beek, L. P. H.: A view on some hydrological triggering systems in landslides,
499 Geomorphology, 30, 25-32, 1999.

500 Van Genuchten, M. T.: A closed-form equation for predicting the hydraulic conductivity of unsaturated soils, Journal of the
501 Soil Science Society of America, 44, 892-898, 1980.

502
503
504
505
506
507
508
509
510

511

512

Table 1 – Historical disasters in Campos do Jordão Municipality. Source: Ridente et al. (2002) and Andrade (2014).

Process	Location	Year	Damages	Causes
Earthflow	Vila Albertina	1972	17 fatalities 60 houses buried	Saturated soil (8m thick), loading and vibration due to construction activities
Landslide	Britador, Vila Santo Antonio and Vila Paulista Popular	1991	149 affected 11 houses buried 4 injured	214.5 mm of rainfall in three days
Landslide and Mudflow	Britador, Vila Albertina, Vila Santo Antônio, Vila Nadir Vila Sodipe and Vila Paulista Popular	2000	10 fatalities 1840 affected	453.2 mm in five days

513

514

515

Table 2 – Results of the geotechnical survey of soils of the study areas.

Sample	Depth (m)	Soil layer	USCS	Unit weight (kN/m ³)	Effective cohesion (kPa)	Effective friction angle (°)	Hydraulic conduct. (m/s)	Gravel (%)	Sand (%)	Silt (%)	Clay (%)	w _L (%)	w _p (%)	IP (%)
SD-01	2.0	R	SC	18.3	37	56	4.44 e ⁻⁶	10	53	25	12	27	18	9
	4.6	S	SC	19.1	18	37	9.46 e ⁻⁶	0	53	35	12	35	22	13
SD-02	6.6	S	SC	17.9	2	49	7.93 e ⁻⁶	0	59	27	14	29	20	9
	2.6	S	SC	21.4	19	34	1.18 e ⁻⁶	5	50	21	24	28	17	11
SD-03	4.6	S	SM	17.5	14	42	3.76 e ⁻⁶	0	73	14	13	33	20	13
	1.6	S	SM-SC	18.1	22	43	5.25 e ⁻⁶	1	59	29	11	22	15	7
SD-05	2.6	S	SM-SC	16.8	2	52	6.13 e ⁻⁷	5	55	30	10	23	17	6
	12.8	S	SC	17.5	48	54	2.77 e ⁻⁷	0	55	33	12	32	21	11
SD-06	7.6	S	SM	17.8	42	28	3.09 e ⁻⁶	1	72	15	12	-	-	-
Block-1	2.0	S	SM	16.0	2	53	9.37 e ⁻⁷	0	72	21	7	-	-	-
Block-2	2.0	S	SM	16.0	49	37	2.98 e ⁻⁶	0	55	42	3	-	-	-
Block-3	3.0	S	SM	16.0	13	46	4.44 e ⁻⁶	0	58	28	14	-	-	-

516

Residual soil (R); Saprolite (S).

517

518

519

520

521

522

Table 3 – Geotechnical and anthropic parameters used on unsaturated seepage and stability analysis

Profile	Geotechnical							Anthropic				
	Slope declivity (°)	Slope height (m)	Soil layers	Shear strength effective parameters#	Unit weight (kN/m ³)#	Rainfall (m/day)	Ksat (m/s)	Pore water pressure (kPa)	Level of the water table	Load in the slope (kN/m ²)	Height of the cut slope (m)	Leaking in the slope (m ³ /day)
A - A'	11 - 40	130										
			Fill Deposit	c' = 2 kPa ϕ' = 31°	14,9		9.50 e ⁻⁶	-7				
B - B'	16 - 33	95	Residual	c' = 15 kPa ϕ' = 36°	18,3	Rainfall events of the 2000 year	4.44 e ⁻⁶	-40	Data of SPT	2.0	6.0	1.0
			Saprolite	c' = 21 kPa ϕ' = 43°	19,1		5.43 e ⁻⁶	-40				
C - C'	15 - 35	87										

Fill Deposit (geotechnical parameters from Ahrendt, 2005)

523

524

525

526

527

528

529

530

531

532

533

534

535

536

537

538

539

540

541

542

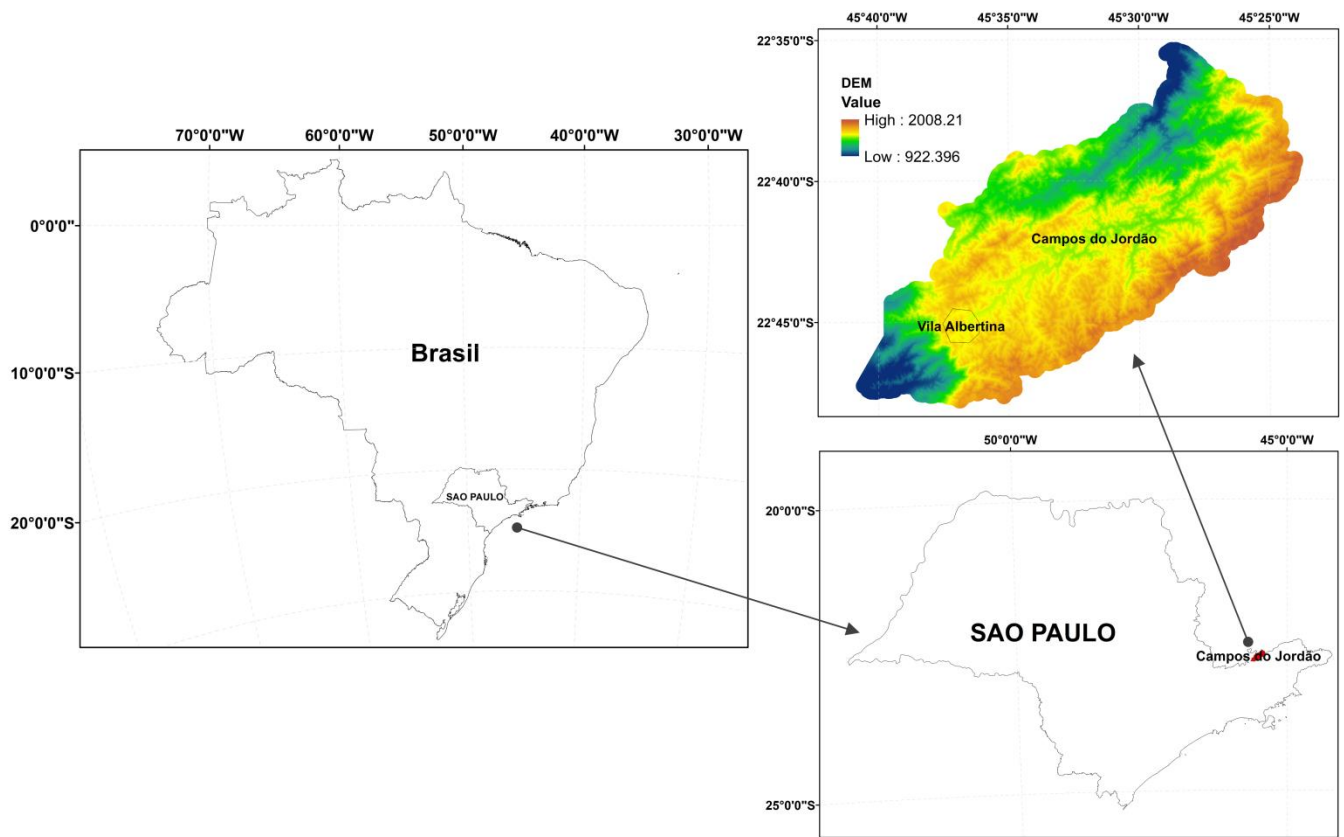


Figure 1. Geographical location of Campos do Jordão municipality and an inset of the study site.

543
 544
 545
 546
 547
 548
 549
 550
 551
 552
 553
 554
 555
 556
 557

558

559



Figure 2. Shallow landslides that happened in 2000 on the study site (Source: Ridente et al., 2002).

560

561

562

563

564

565

566

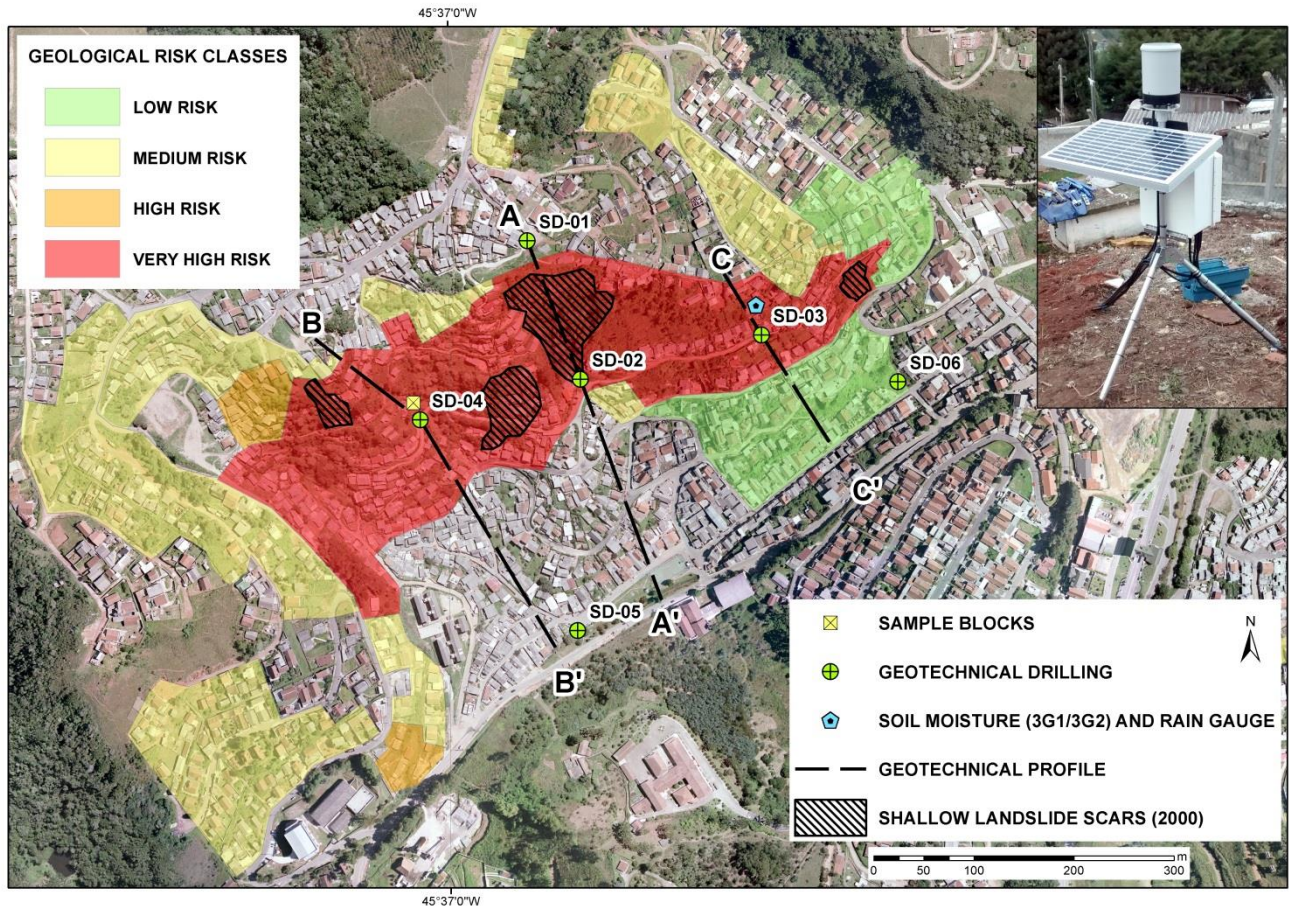
567

568

569

570

571



573
574
575
576

Figure 3. Satellite image of the study site showing the location of monitoring instruments (symbols), geotechnical transects (dotted lines along the slopes); landslide susceptibility areas indicating the level of risk (areas shaded in yellow, orange and red); scars of previous shallow landslides (black cross-hatched area).

577
578
579
580
581
582
583
584
585
586

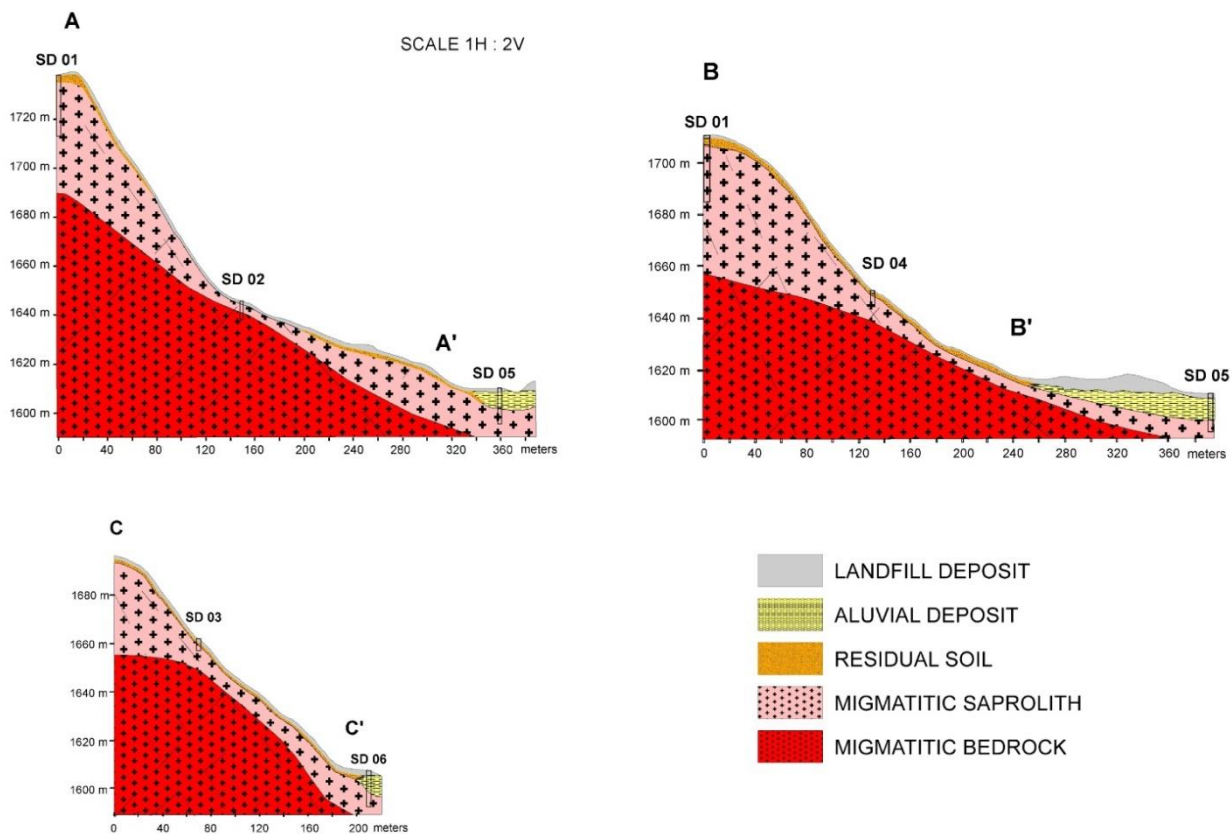


Figure 4. Geological-geotechnical profiles of the study area derived from the geotechnical survey.

588

589

590

591

592

593

594

595

596

597

598

599

600

601

602

603

604

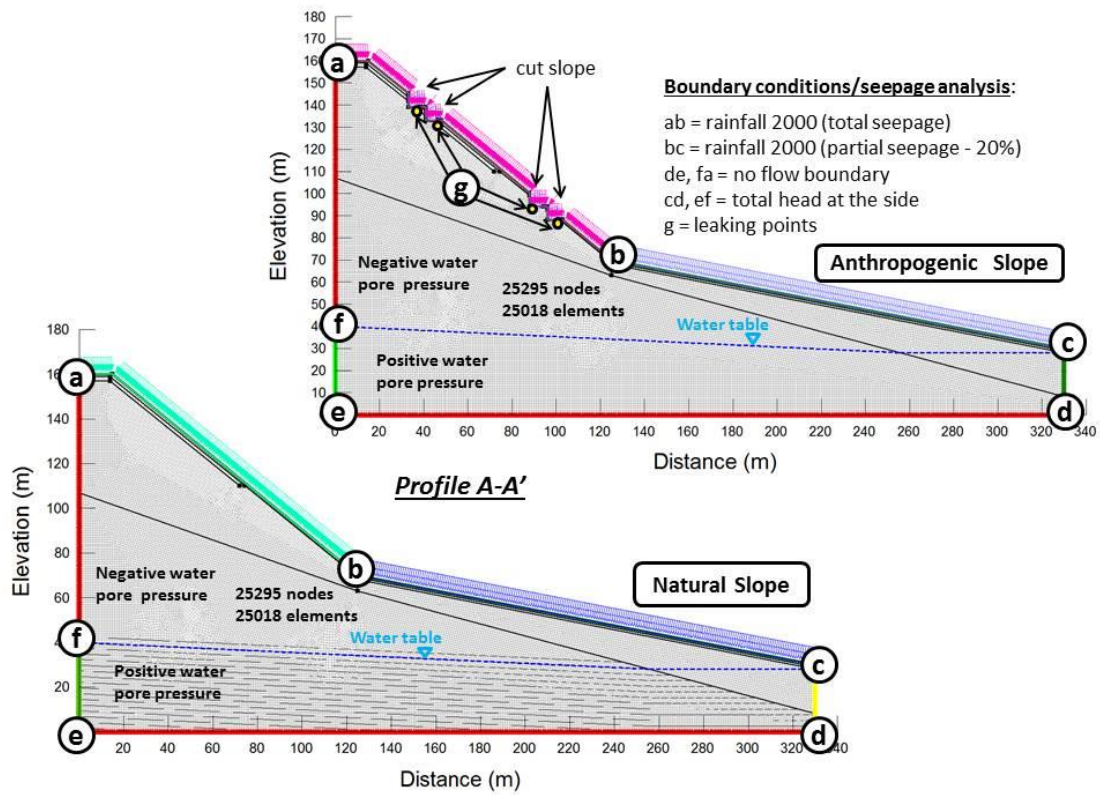


Figure 5. Slope geometry and boundary conditions used in the unsaturated transient seepage analysis considering natural and anthropogenic factors (rainfall, cut slope and leakage).

606

607

608

609

610

611

612

613

614

615

616

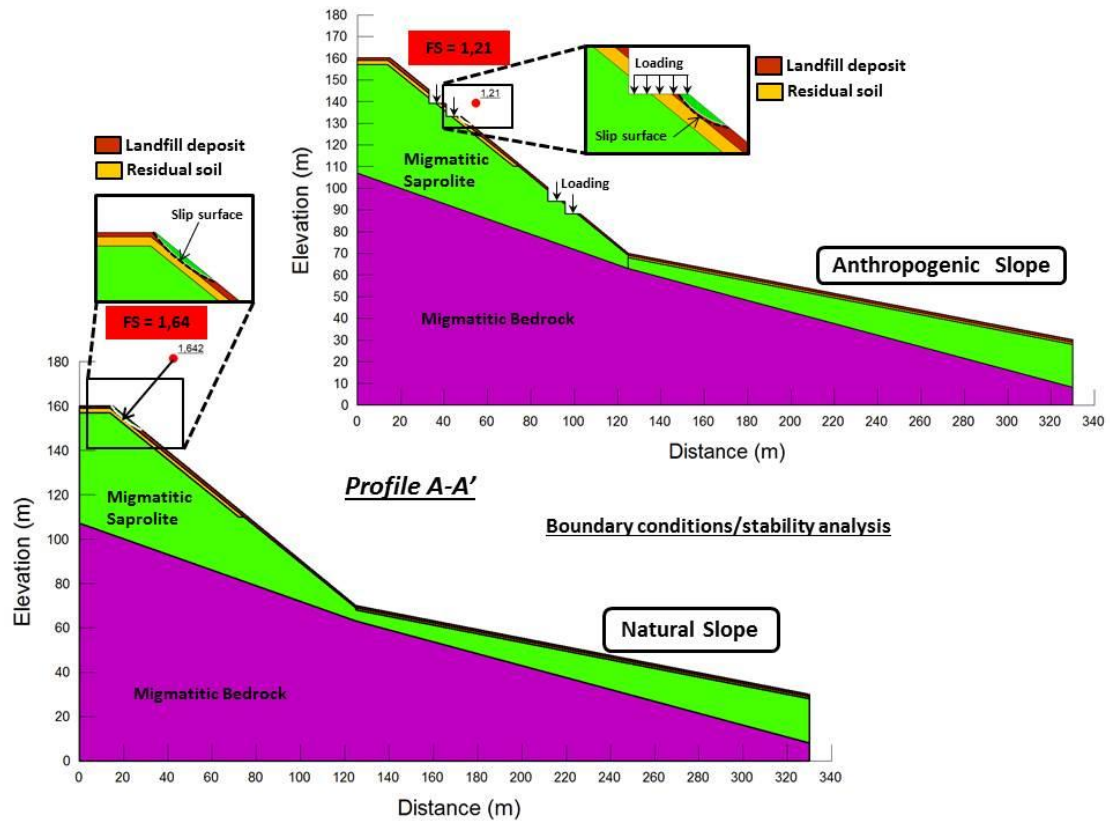
617

618

619

620

621



623

624

Figure 6. Slope geometry and boundary conditions used in the stability analysis considering natural and anthropogenic factors (rainfall, cut slope, loading and leakage).

625

626

627

628

629

630

631

632

633

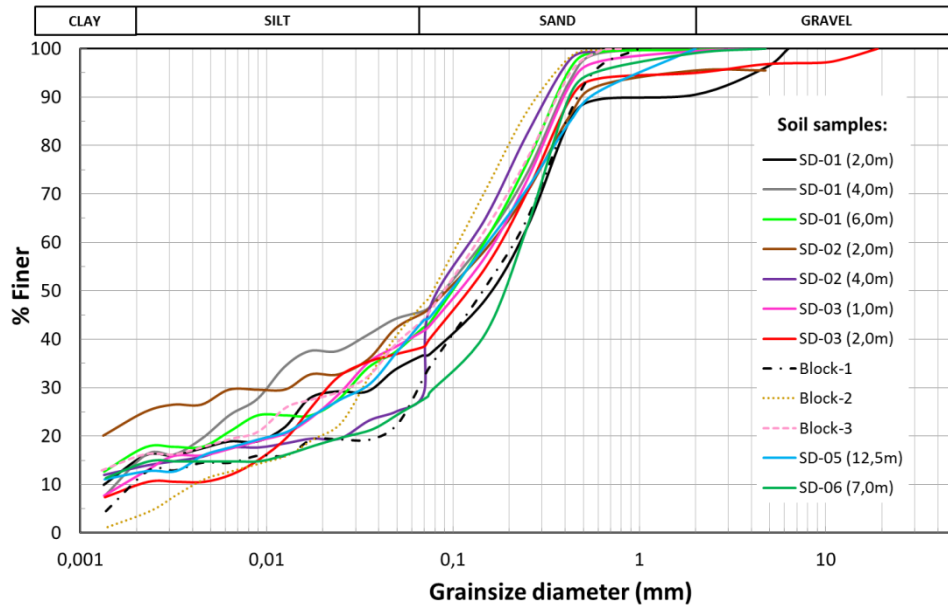
634

635

636

637

638



640

641

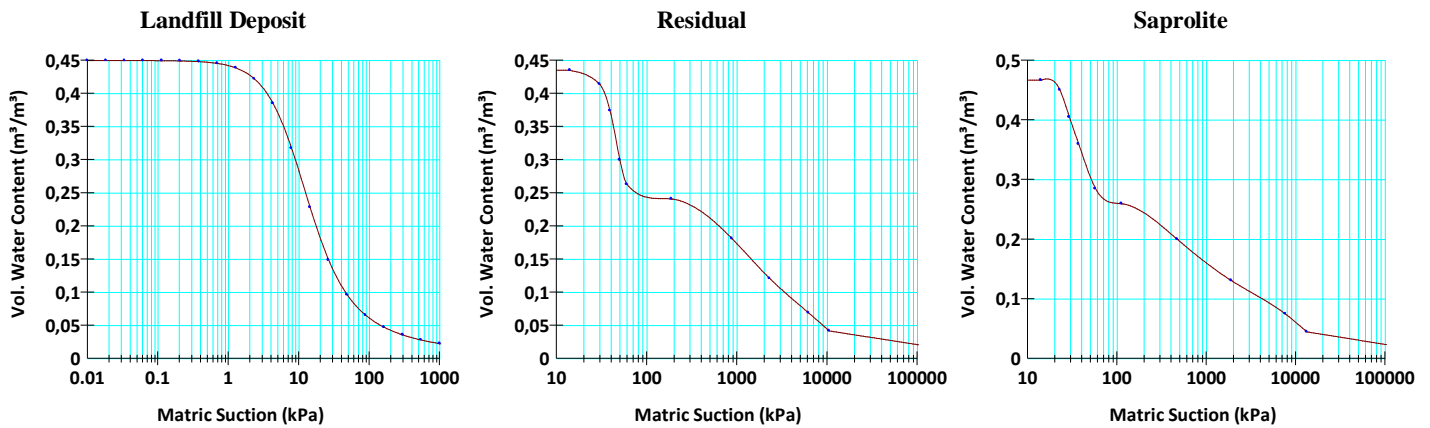
642

643

644

645

Figure 7. Granulometric distribution for the residual soil and the saprolite of the six boreholes analysed (SD-01 to SD-06) and for the undisturbed soil cores (Block-1 to Block-3).



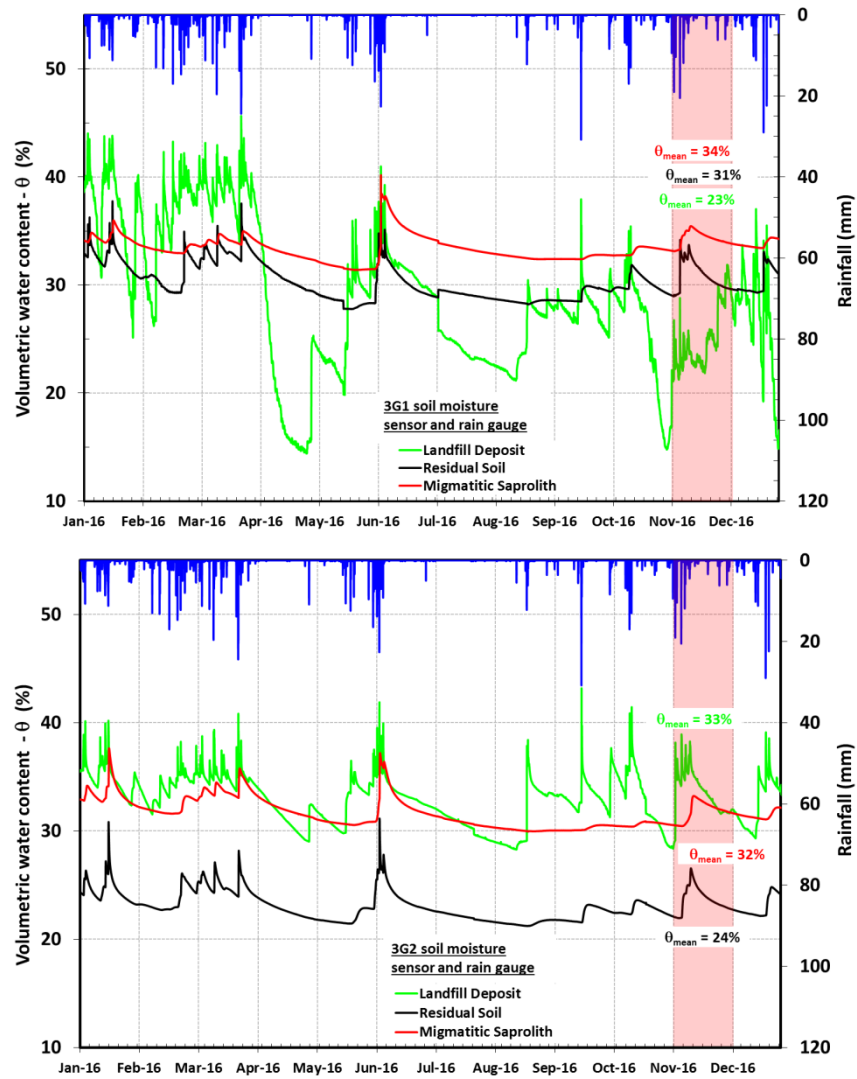
646

647

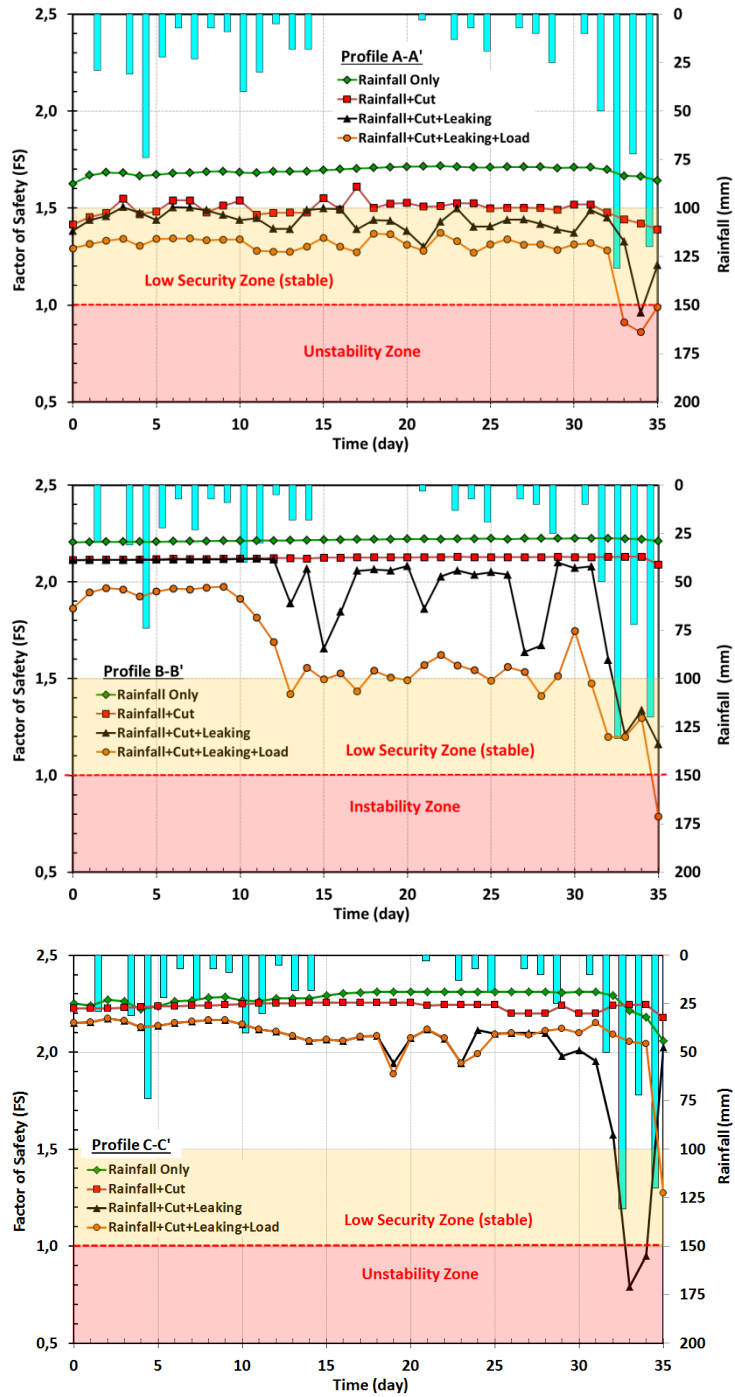
648

649

Figure 8. Water retention curves of the three soil types used in transient seepage analysis.



651 **Figure 9.** Time variation of soil moisture at different depths during 2016 in the study area in the sensor 3G1 (upper graph) and 3G2
 652 (bottom graph).
 653
 654
 655
 656
 657
 658
 659



660 **Figure 10.** Time variation of the slope safety factor for natural conditions and taken into account the additional effects introduced by
 661 anthropic disturbances on profiles A-A', B-B' and C-C'.
 662